J Mater Sci: Mater Med (2007) 18:819–827
DOI 10.1007/s10856-006-0015-z

Characterisation of wear particles produced by metal on metal and ceramic on metal hip prostheses under standard and microseparation simulation

Christopher Brown · Sophie Williams · Joanne L Tipper · John Fisher · Eileen Ingham

Received: 18 May 2005 / Accepted: 29 December 2005 / Published online: 14 December 2006

Abstract The failure of metal on polyethylene total hip replacements due to wear particle induced osteolysis and late aseptic loosening has focused interest upon alternative bearings, such as metal on metal implants. A recent advance in this field has been the development of a novel ceramic on metal implant. The characteristics of the wear particles generated in this low-wearing bearing have not been previously determined. The aims of this study were to characterise metal wear particles from metal on metal and ceramic on metal hips under standard and adverse (microseparation) wear conditions. Accurate characterisation of cobalt-chrome wear particles is difficult since the reactive nature of the particles prevents them from being isolated using acids and bases. A method was developed to isolate the metal wear particles using enzymes to digest serum containing lubricants from metal on metal and ceramic on metal hip simulations. High resolution scanning electron microscopy was then used to characterise the wear particles generated by both metal on metal and ceramic on metal implants under standard and microseparation wear conditions. The wear particles isolated from all simulations had a mean size of less than 50 nm with a rounded and irregular morphology. No significant difference was found between the size of wear particles generated under any conditions.

C. Brown (✉) · S. Williams · J. L. Tipper · J. Fisher · E. Ingham
Institute of Medical and Biological Engineering, University of Leeds, LeedsWoodhouse Lane, West Yorkshire LS2 9JT, UK
e-mail: mencbr@leeds.ac.uk

1 Introduction

In the UK there are approximately 50,000 total hip replacements (THR) carried out every year and world wide the number is as great as 800,000. The most commonly implanted prosthesis type consists of an ultra high molecular weight polyethylene (UHMWPE) cup articulating upon a highly polished metal or ceramic femoral head [1]. Initially, this was believed to be a more than adequate replacement for damaged joints however, some studies have reported a failure rate of 60% due to periprosthetic osteolysis at 12 years [2]. Conversely, a significant number of metal on metal implants survived for over 20 years with little incidence of osteolysis or late aseptic loosening [3]. These findings coupled with the need to find a replacement for implants with UHMWPE bearings has rekindled interest in the use of metal bearing surfaces.

One advantage of metal on metal prostheses is their low wear rates with implants shown clinically to be capable of producing wear rates as low as 0.3 $mm^3/10^6$ cycles [4]. Studies have also indicated that the size of wear particles produced by metal on metal implants in vivo is in the nanometre size range thus reducing the potential for the induction of osteolysis [5]. However, the small size of the wear particles may facilitate their dispersal via the lymphatic system to sites distant from the implant and it has been reported that cobalt-chrome particles can accumulate in the liver, spleen, lymph nodes and bone marrow of patients [6, 7]. This, together with the reactive nature of metallic particles has led to concerns about their potential to cause cytotoxicity [8–10], hypersensitivity [11, 12] and neoplasia [13–15].

In addition to particle size, another important factor that may influence the biological effects of wear particles in vivo is the volume of particles generated. Thus, any reduction of wear will be highly favourable in the longer-term. To this end, a novel ceramic on metal implant has been developed [16]. Firkins et al. [16] reported on the wear of the ceramic on metal prosthesis in a hip joint simulator and found a wear rate of 0.01 $mm^3/10^6$ cycles. Thus, this bearing has the potential for a greater than 10-fold reduction of wear compared to metal on metal implants. This is thought to be a result of the differential hardness of the ceramic on metal bearing, the benefits of which are a reduction in adhesive wear and that wear only occurs to one bearing surface. To date, however, there has been limited study of the wear particles produced by ceramic on metal implants [16].

The majority of cobalt-chrome wear particles that were isolated by Doorn et al. [5] from metal on metal retrieval tissues were round in shape, with some shard or needle-like particles observed, and ranged in size from 51–116 nm with a mean size of 81 nm. The size of particles generated in vitro in metal on metal hip simulations, 25–36 nm [17], has been shown to be similar to those seen in vivo, however the morphology of particles generated in vitro differs to those produced *in vivo*. Firkins et al. [17] used TEM and showed that the morphology of particles produced in a physiological simulator by metal on metal articulations displayed little variation and was mostly oval or rounded in shape with no shard-like debris observed. One explanation for this difference in morphology provided by the author was that the simulator testing only provided a best case wear scenario [17]. Hip simulator studies have been designed to incorporate microseparation in order to produce wear rates and patterns in vitro that compare with those observed in vivo for ceramic on ceramic bearings [18, 19] and metal on metal bearings [20]. For ceramic on ceramic bearings, microseparation resulted in the production of particles with a bimodal size distribution [21]. For metal on metal, the introduction of microseparation resulted in no change in the particles which were 6–15 nm in size [20]. However, in this study particles were analysed using TEM which as indicated below may have limitations. There have been no previous studies of the particles produced by ceramic on metal bearing under adverse simulation conditions.

The study of particles generated by metal on metal implants is further complicated by the reactive nature of metal particles. Catelas et al. [22; 23] demonstrated that the use of alkaline digestion to isolate metal particles could significantly alter the size of particles generated in simulators and pin-on-plate wear tests whilst the use of enzymes to isolate particles was not found to alter the particle's chemical composition [23]. Yanez et al. [24] also highlighted the problems associated with trying to resolve small particles by SEM. They showed that the use of high accelerating voltages (kV) to improve the resolution of SEM can cause errors in particle area measurement. Doorn et al. [5] used TEM to analyse the metal wear particles generated *in vivo* whilst Williams et al. [20] used TEM to analyse metal particles from hip joint simulations. There are a number of considerations, though, that must be taken into account when using TEM for particle analysis. Wear particles may be unevenly distributed and only a small amount of the sample is investigated leading to inaccurate sampling. The methods used to prepare the particles for TEM can cause them to aggregate making accurate analysis difficult and also larger particles can be removed from the sample completely.

The aims of this study were to develop a novel method for the isolation and comparison of wear particles from metal on metal and ceramic on metal hip simulations by combining the use of a novel enzymatic digestion technique with a field emission gun scanning electron microscope (FEGSEM) capable of producing high resolution images. In addition, wear particles generated by metal on metal and ceramic on metal prostheses under standard and adverse (microseparation) wear conditions were isolated and compared in order to investigate whether these factors influenced particle size.

2 Materials and methods

2.1 Metal on metal articulations

The prostheses used in this study were manufactured from medical grade wrought cobalt chrome alloy (ASTMF1537) and comprised 28 mm femoral heads and acetabular cups (De Puy International, Leeds, United Kingdom). The femoral heads were made from low carbon content alloy (< 0.07 %) whilst the acetabular cups comprised high carbon content alloy (> 0.2 %). These cups were mounted into titanium shells which in turn were mounted into simulator cup holders and had an identical mean diametrical clearance of 50 μm. The articulating surface of each bearing was finished to give a mean surface roughness (R_a) of approximately 0.02 μm.

2.2 Ceramic on metal articulations

The femoral heads used in this study were manufactured from medical grade HIPed alumina (ISO 6474)

BIOLOX FORTE (Ceramtec) and had a diameter of 28 mm. The heads were coupled with 28 mm acetabular cups made from medical grade high carbon (> 0.2 %) wrought cobalt chrome alloy (ASTMF1537, De Puy International, Leeds, United Kingdom). The heads and cups were mounted in an identical manner to the metal on metal prostheses. The femoral heads were mounted onto tapered spigots of the femoral stems. The bearings had a diametrical clearance of 60 μm whilst the articulating surface of each bearing was finished to give a mean surface roughness (R_a) of 0.02 μm.

2.3 Wear particle generation under standard wear conditions

Wear particles were generated under standard wear conditions in the Leeds Mark II Physiological Anatomical (PA) hip simulator for both ceramic on metal and metal on metal bearing combinations. Barbour et al. [25] and Firkins et al. [17] have both shown that this simulator can produce wear rates similar to those observed in vivo for UHMWPE on metal and metal on metal respectively.

The simulator was a 3-axis machine in which the inserts were positioned superiorly to the heads at an incline of 45° to the vertical axis. The vertical load applied through the simulator had a twin peak and followed a ''Paul-type'' loading cycle. This loading cycle demonstrated two peaks of 3 kN which corresponded to heel-strike and toe off. These peaks were separated by a 1 kN trough which represented stance phase and was smoothly applied for 65% of the cycle time. A residual force of 270 N, during swing phase, was applied for the remainder of the cycle. The vertical load was combined with two independently controlled axes of motion: internal/external rotation and flexion/extension. These cycles were simplified in order to generate multi-directional motion between the acetabular cup and femoral head.

The simulations were run for five million cycles at a frequency of 1 Hertz in a lubricant comprising 25% (v/v) bovine calf serum (BCS). Sodium azide (0.1%; v/v) was added to the lubricant to limit the level of bacterial growth. At every 0.33 million cycles the lubricant was removed and then stored at –18°C.

2.4 Wear particle generation under microseparation wear conditions

Microseparation wear conditions were implemented to replicate a small amount of separation of the hip during swing phase of gait. A full description of the method can be found in Williams et al. [20]. Wear particles were generated under microseparation wear conditions in a ten station Prosim (Manchester, UK) hip simulator for both ceramic on metal and metal on metal bearing combinations. The simulator had two independently controlled axes of rotation and a single axis of loading. A flexion-extension motion was applied to the femoral head in a modified sine wave with amplitude of +30–15°. Internal–external rotation was applied to the acetabular cup as a sine wave with amplitude of ±10°. Both motions were applied at identical frequencies but 270° out of phase [20].

The loads applied to this simulator were of a ''Paul-type'' as described in above. However in order to achieve microseparation it was necessary to modify the loading cycle. An actuator was used to apply an inferior load to the femoral head. During swing phase this caused the femoral head and acetabular cup to separate by approximately 0.8 mm. The separation of the two components led to contact of the head with the inferior rim of the cup. In turn, this caused lateral displacement of the femoral head as it tracked around the rim. Upon heel strike a load was applied again which resulted in the head translating superiorly and making contact with the rim of the cup before relocating into the centre of the cup [20].

The simulations were run for five million cycles at a frequency of 1 Hertz in a lubricant comprising 25% (v/v) BCS. Sodium azide (0.1%; v/v) was added to the lubricant to limit the level of bacterial growth. At every 0.33 million cycles the lubricant was removed and then stored at –18°C.

2.5 Isolation of wear particles from serum containing lubricant

Three samples of serum lubricant (200 ml) were taken from each hip joint simulation and centrifuged at 15,000 g for 20 min. The supernatant was removed and the pellets (containing particles, precipitated proteins and microbes) were rehydrated for 18 h in 5 ml of 0.05% sodium azide (w/v) in 3-(N-morpholino) propanesulphonic acid (MOPS; 0.1 M, pH 6.5) buffer. The proteins were denatured by boiling the samples for 10 min in 5 ml of MOPS containing 5% (w/v) β-mercaptoethanol and 2% sodium dodecyl sulphate (w/v, SDS). The samples were then centrifuged at 11,000 g for 10 min and the supernatant containing denatured proteins was removed. The pelleted samples were then boiled for 10 min in 5 ml of 2 % (w/v) SDS in MOPS only and were then washed sequentially in 5 ml of MOPS, 5 ml of 80% (v/v) acetone and then 5 ml of MOPS solution. The samples were sonicated in a sonic bath for 30 min in 1 ml of MOPS buffer

containing Tris(2-carboxyethyl)–phosphine (TCEP; 9 mM) before 7.6 μl of papain (P-3125, Sigma-Aldrich) was added giving a final concentration of 0.21 mg.ml^{-1}. Samples were digested for 3 h at 55°C and this step was repeated 3 times. The samples were then boiled in 2% (w/v) SDS in MOPS for 10 min and then washed in MOPS solution prior to being sonicated for 30 min in 5 ml of 50 mM Tris–HCl (pH 7.8). Proteinase K (1.7 mg, 39037, VWR International) was then added to the samples to give a final concentration of 0.34 mg.ml^{-1} and the samples were subjected to enzymatic digestion at 55°C for 3 h This step was repeated three times. The samples were then boiled in 2% (w/v) SDS for 10 min and were then washed in MOPS solution. Samples were then resuspended in 1 ml of 1.1 M sorbitol in HEPES buffer (pH 7.4) containing yeast lytic enzyme (20 U.ml^{-1}, YLE, 155270, ICN Pharmaceuticals) and digested for 2 h at 37°C. This step was repeated 3 times. The samples were then boiled in 2% (w/v) SDS for 10 min and then washed in MOPS buffer prior to being digested in 1 ml of Zymolyase 100 T (250 U.ml^{-1}, 120493^{-}1, ams Biotechnology (Europe)) in 0.1 M sodium phosphate buffer (pH 7.0) containing 50 mM (v/v) β-mercaptoethanol. The samples were digested for 2 h at 37°C. This was repeated three times. The samples were then boiled in 2% (w/v) SDS for 10 min and then washed in MOPS buffer prior to being digested for 2 h in 1 ml of proteinase K solution at 55°C. This was repeated three times. Particles were then washed five times in filtered deionised water and sonicated for 1 min in 5 ml of filtered deionised water before being heated to 180°C for 4 h Particles were then sonicated for 1 min in Elmaclean 65 solution and then washed three times in filtered deionised water. Following digestion, the particles were sequentially filtered onto 5, 1 and 0.1 μm polycarbonate 25 mm diameter filters and dried for 4 h.

2.6 Characterisation of wear particles from hip simulations

A section approximately 0.5 cm^2 was taken from an area between the edge and the middle of each 5, 1 and 0.1 μm filter for each sample of wear particles. These portions were then coated with 5 nm of Pt/Pd and viewed and analysed by EDX using a LEO FEGSEM. Images were generated and were then analysed using Image Pro Plus® imaging software whilst Link ISIS® software was used to perform EDX. Three replicates were analysed for each material combination and measurements from all filter sizes were combined to generate size distributions. Only images of magnifications greater than 125,000 × magnification were assessed.

2.7 Statistical analyses

Maximum diameter measurements were taken for 150 particles per sample to generate size distributions. The size of the particles generated under each of the various conditions was compared by one-way ANOVA. The minimum significant difference (MSD; $p < 0.05$) between group means was calculated using the T-method.

3 Results

3.1 Characterisation of wear particles by high resolution microscopy

The use of the FEGSEM allowed resolution of particles to 5 nm. The wear particles isolated from metal on metal implants under standard wear conditions at one million cycles in serum containing lubricant were found to range between 8 and 116 nm in size with a rounded and irregular morphology (Fig. 1a; 1b). The wear particles isolated from metal on metal implants under microseparation wear conditions in serum containing lubricant after 1.5 million cycles were found to range between 8 and 107 nm in size with a rounded and irregular morphology (Fig. 1c). The wear particles isolated from metal on metal implants under microseparation wear conditions in serum containing lubricant after four million cycles were in the same size range (6–146 nm) with a similar morphology (Fig. 1d). Under standard conditions, the wear particles isolated from ceramic on metal implants at one million cycles were between 8 and 139 nm in size and also had a rounded and irregular morphology (Fig. 1e).

Under microseparation, the wear particles isolated from ceramic on metal implants after 1.5 million cycles were in the same size range (7–156 nm) with the same morphology (Fig. 1f).

The wear particles isolated from ceramic on metal implants under microseparation wear conditions in serum containing lubricant after four million cycles were 8–140 nm in size again with a rounded and irregular morphology (Fig. 1g).

3.2 Distribution of wear particles as a function of size

The frequency distributions as a function of size of the particles generated under the different simulations are presented in Fig. 2. The wear particles isolated from metal on metal implants under standard wear

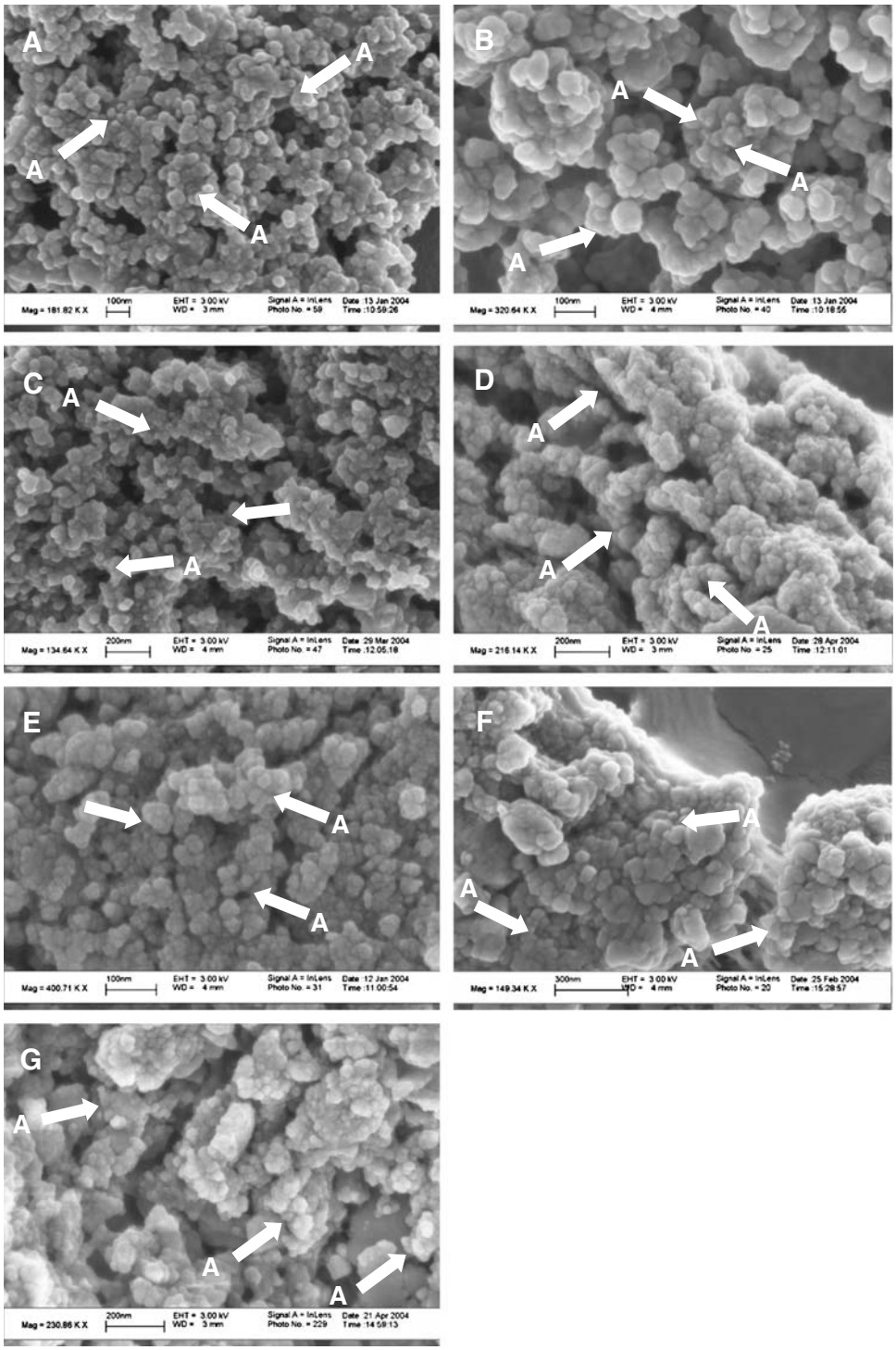

Fig. 1 FEGSEM Images of Particles. (a, b) Particles generated by a metal on metal implant under standard wear conditions in serum containing lubricant after one million cycles. Viewed at 182,820 × and 320,640 × magnification respectively. (c) Particles generated by a metal on metal implant under microseparation wear conditions in serum containing lubricant after 1.5 million cycles. Viewed at 134,640 × magnification. (d) Particles generated by a metal on metal implant under microseparation wear conditions in serum containing lubricant after four million cycles. Viewed at 216,140 × magnification. (e) Particles generated by a ceramic on metal implant under standard wear conditions in serum containing lubricant after one million cycles. Viewed at 400,710 × magnification. (f) Particles generated by a ceramic on metal implant under microseparation wear conditions in serum containing lubricant after 1.5 million cycles. Viewed at 149,340 × magnification. (g) Particles generated by a ceramic on metal implant under microseparation wear conditions in serum containing lubricant after four million cycles. Viewed at 230,860 × magnification. A = CoCr particles

conditions at one million cycles had a mode of distribution in the 30–39 nm size range with a mean size of 34.72 nm (Fig. 2a).

The wear particles isolated from metal on metal implants under microseparation wear conditions after 1.5 and 4 million had a mode of distribution in the 20–29 nm size range with mean sizes of 35.62 and 31.16 nm respectively, (Fig. 2b and 2c).

The wear particles isolated from ceramic on metal implants under standard wear conditions at one million cycles had a mode of distribution in the 20–29 nm size range with a mean size of 36.67 nm (Fig. 2d).

The wear particles isolated from ceramic on metal implants under microseparation wear conditions after 1.5 and 4 million had a mode of distribution in the 20–29 nm size range with mean sizes of 41.29 nm and 33.59 nm respectively (Fig. 2e and 2f).

3.3 Characterisation of wear particles by EDX

Analysis by EDX of the wear particles isolated from all of the simulations showed the particles to be cobalt, chromium and molybdenum. Examples of the data for

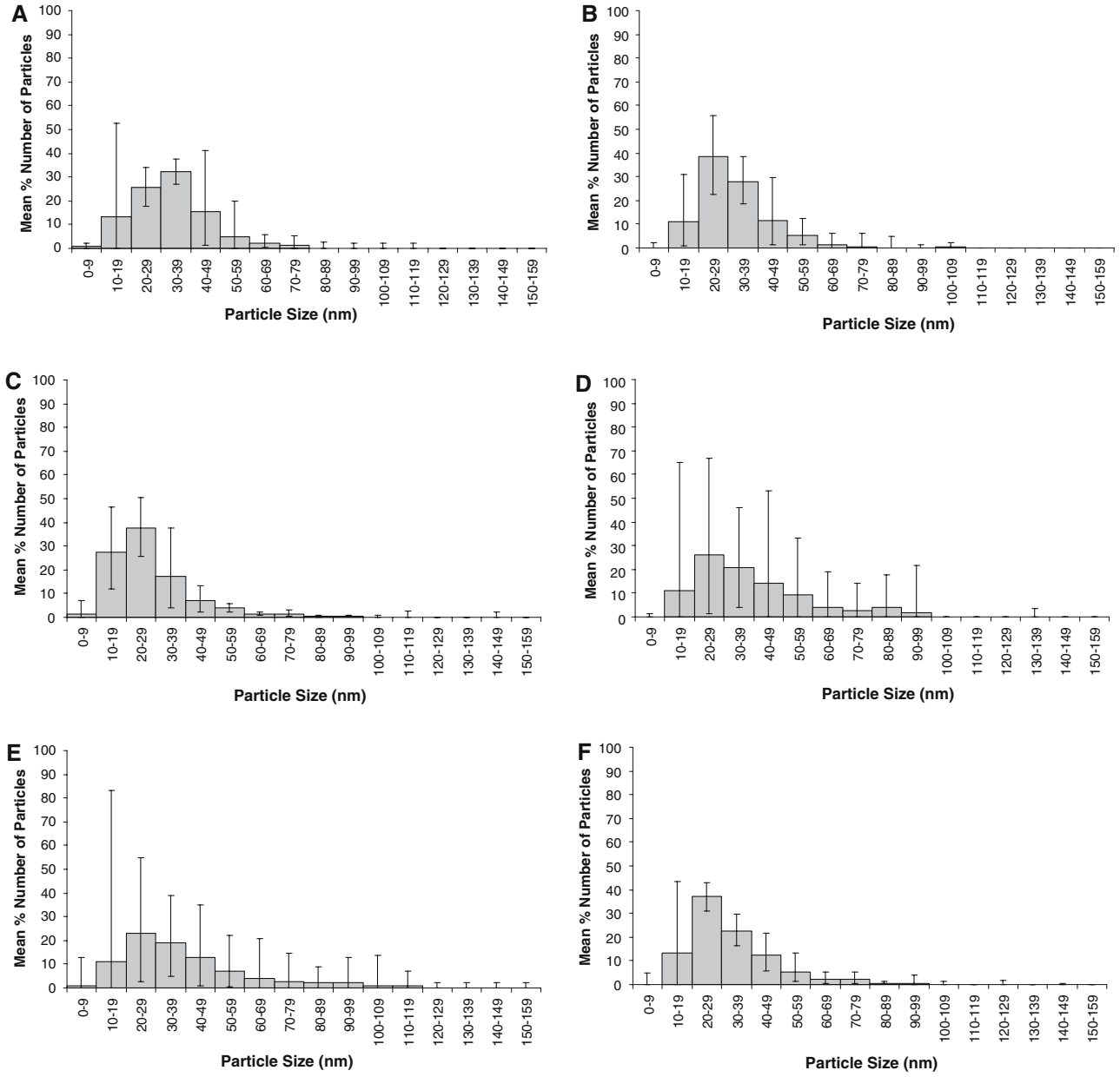

Fig. 2 Frequency distribution as a function of particle size for wear particles generated by: (a) metal on metal implants under standard wear conditions in serum containing lubricant after one million cycles. (b) Metal on metal implants under microseparation wear conditions in serum containing lubricants after 1.5 million cycles. (c) Metal on metal implants under microseparation wear conditions in serum containing lubricants after four million cycles. (d) Ceramic on metal implants under standard wear conditions in serum containing lubricant after one million cycles. (e) Ceramic on metal implant under microseparation wear conditions in serum containing lubricant after 1.5 million cycles. (f) Particles generated by a ceramic on metal implant under microseparation wear conditions in serum containing lubricant after four million cycles. One hundred and fifty particles were analysed from each of three replicate samples of lubricant. Data (%) was arcsin transformed and 95% confidence limits calculated. Data was back-transformed to percentages for presentation.

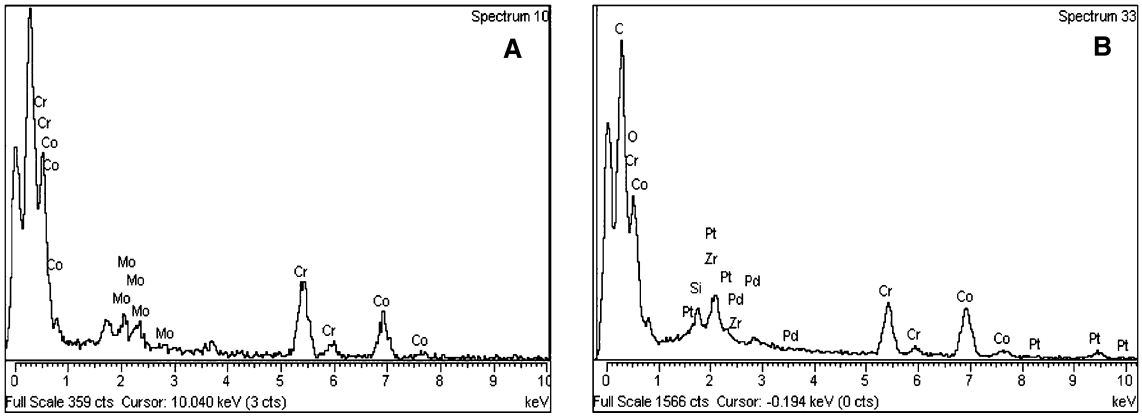

Fig. 3 EDX of Particles Generated by: (a) Metal on metal implants under standard wear conditions in serum containing lubricant. (b) Ceramic on metal implants under standard wear conditions in serum containing lubricant. Spectra show presence of CoCr particles

metal on metal and ceramic on metal are presented in Fig. 3.

3.4 Comparison of wear particles generated by metal on metal and ceramic on metal implants under standard and microseparation wear conditions in serum containing lubricants and water

A summary of the results for each simulation condition for the metal on metal and ceramic on metal articulations is presented in Table 1. The data was analysed by one-way ANOVA which revealed no significant difference in the particle size generated by the two bearing types when tested under standard or microseparation wear conditions ($p > 0.05$).

4 Discussion

This study has been the first to successfully isolate and characterise the wear particles from both metal on metal and ceramic on metal implants generated under both standard and microseparation wear conditions from hip simulators in serum lubricants. The development of a novel enzymatic digestion technique to isolate the metal particles avoided the use of acids or bases thus preventing damage of the particles during isolation and wear particles could be clearly resolved and characterised. The use of the FEGSEM generated images at magnifications in excess of 100,000 times at accelerating voltages as low as 3 kV. The high resolving power of the FEGSEM allowed for particles to be accurately characterised whilst distortion of the size and shape of particles was reduced by the low accelerating voltages.

Characterisation of the wear particles generated in hip simulators revealed no significant difference in particle morphology or size distribution for any of the bearing combinations regardless of the wear conditions or number of wear cycles. Particles were found to be rounded and irregular in shape and were typically less than 40 nm in size with more than 95 percent of particles under 100 nm in size. This study has shown that there is no significant difference between the metal wear particles generated by either metal on metal or

Table 1 Comparison of wear particles generated by metal on metal and ceramic on metal implants under standard and microseparation wear conditions in serum containing lubricants and water

Bearing Combination	Lubricant	Wear Condition	No. of Cycles (million)	Mean Size (nm) ± 95% CL	P-value vs. other groups
Metal on metal	Serum	Standard	1	34.72 ± 1.29	ns
Metal on metal	Serum	Microseparation	1.5	35.62 ± 1.47	ns
Metal on metal	Serum	Microseparation	4	31.16 ± 1.82	ns
Ceramic on metal	Serum	Standard	1	36.67 ± 1.76	ns
Ceramic on metal	Serum	Microseparation	1.5	41.29 ± 2.25	ns
Ceramic on metal	Serum	Microseparation	4	33.59 ± 1.47	ns

Mean particle size is shown in nanometres (nm; $n = 3$). Data was analysed by one-way ANOVA and calculation of the MSD by the *T*-method. Wear particles with a mean not significantly different from the other groups are indicated by 'ns'

ceramic on metal under standard or microseparation wear conditions. This is in contrast with the results of studies of the effects of microseparation upon ceramic on ceramic implants in which it was found that microseparation in vitro produced particles with a bimodal size distribution with both nanometre and micrometre particles being generated [21]. The difference between these two bearings is possibly due to the differing material properties. Ceramics are more brittle than metal and may fracture under harsh wear regimes due to joint laxity whereas, with ceramic on metal even under microseparation conditions, wear occurs on the softer, metallic component. The lack of a difference in particle size distribution between metal on metal and ceramic on metal implants under standard and microseparation wear conditions suggests that ceramic on metal implants may be better suited than ceramic on ceramic implants for use by young and active patients as they fail to generate particles in the critical size range for macrophage activation [26] and have a lower potential to induce osteolysis.

Previous studies that have characterised the wear particles present in the tissues surrounding metal on metal implants have found these wear particles to range from 10 nm to 5 μm in size [5, 6, 27–30]. The wear particles observed in these studies were often rounded granules less than 50 nm in size. However, the authors also noted larger shards and needle-like particles. The most recent of these studies, Doorn et al. [5], used TEM to characterise metal wear particles generated in vivo. They reported that the majority of particles were rounded and ranged in size from 51–116 nm with a mean size of 81 nm. In contrast the particles generated by the metal on metal implants under standard and microseparation wear conditions were found to range from 6–149 nm in size with mean sizes less than 40 nm. Also, the particles were found to have a round morphology and no shard or needle-like particles were observed. The disparity in these results may be due to a number of reasons. Firstly, the use of TEM by Doorn et al. [5] would not produce images with as high a resolution as the FEGSEM. This could, therefore, have resulted in less accurate sizing of particles which may have aggregated. Secondly, even under microseparation wear conditions the hip simulators may still result in a best case wear scenario as described previously by Firkins et al. [16]. The shard and needle-like particles observed in ex vivo studies may be due to ranges of motion in vivo that are not replicated by the hip simulators. Thirdly, the large particles observed in previous studies may have been due to the use of acids and bases in the isolation of these particles. Catelas et al. [22, 23] found that the use of these chemicals to isolate metal particles could alter the morphology of the wear particles and it may also have caused the particles to become aggregated. The particle isolation technique used in this study avoided acids or bases in order to minimise morphological changes. The repeated boiling of the particles in MOPS containing 5 % (w/v) β-mercaptoethanol and 2% (w/v) SDS did not have an adverse affect, as the particles isolated in this study displayed no significant difference in size or morphology to those observed without isolation from serum containing lubricant [16]. A final explanation for the disparity between the two results maybe the difference in grain size present in wrought and cast bearings. It has been suggested that wear particle generation in metal on metal implants may be due to fatigue of martensitic bands and at high contact pressures the grain size of the bearing surfaces could influence the aspect ratio of the particles generated [31]. This study has investigated metal on metal prostheses manufactured from wrought cobalt-chrome whilst Doorn et al. [5] investigated tissues from patients with implants manufactured from cast cobalt-chrome. As the grain sizes in cast cobalt-chrome are larger than those present in the wrought material the martensitic bands are also larger and so shard-like particles are more likely to be produced by the cast bearings. High carbon content wrought cobalt-chrome also has a smaller grain size than the low carbon wrought alloy and so may produce fewer needle shaped particles. The combination of a low carbon cobalt chrome femoral head and high carbon acetabular cup in metal on metal implants leads to wear originating from the low carbon alloy. Although no difference was found between metal on metal and ceramic on metal implants in this study the use of high carbon content cobalt chrome as a bearing surface in ceramic on metal implants may result in some difference in particle morphology by the two types of implants in vivo. However, clinical studies with ceramic on metal are at an early stage and there are no studies of the wear particles generated by these implants in vivo.

In simulator studies ceramic on metal implants have been found to have wear rates of 0.01 mm^3 per million cycles compared with 0.1 mm^3 per million cycles found in metal on metal implants [16]. As metal on metal and ceramic on metal implants have been shown to generate wear particles of a similar shape and size, the concerns about cytotoxicity, hypersensitivity and neoplasia which are associated with metal particles will also apply to ceramic on metal implants. However, the ten-fold lower wear rate of ceramic on metal implants would have a great advantage over metal on metal implants, as over a given time period, they would be

expected to produce 10-fold fewer wear particles than metal on metal implants. Therefore, the potential for long-term problems with ceramic on metal implants will be greatly reduced.

Acknowledgments This research was supported by a case studentship from the EPSRC and Depuy International, Leeds, UK. Thanks go to John Harrington for his help with the FEGSEM.

References

1. E. INGHAM and J. FISHER,*Proc. Instn. Mech. Engrs*. **214** Part H (2000) 21
2. W. H. HARRIS, *Clin. Orthop.* **393** (2001) 66
3. H. C. AMSTUTZ, P. A. CAMPBELL, H. A. MCKELLOP, T. P. SCHMALZREID, W. J. GILLESPIE, D. W. HOWIE, J. J. JACOBS, J. B. MEDLEY, K. MERRITT, *Clin. Orthop*. **329S** (1996) S297
4. H. P. SIEBER, C. B. RIEKER, P. KOTTIG, *J. Bone Joint Surg*. 81 (1999) 46
5. P. F. DOORN, P. A. CAMPBELL, J. WORRALL, P. D. BENYA, H. A. MCKELLOP, H. C. AMSTUTZ, *J. Biomed. Mater. Res*. **42** (1998) 103
6. C. P. CASE, V. G. LANGKAMER, C. JAMES, M. R. PALMER, A. J. KEMP, P. F. HEAP, L. SOLOMAN, *J. Bone Joint Surg*. **76B** (1994) 701
7. R. M. URBAN, J. J. JACOBS, M. J. TOMLINSON, J. GAVRILOVIC, J. BLACK, M. PEOC'H, *J. Bone Joint Surg*. **82A** (2000) 457
8. L. SAVARINO, D. GRANCHI, G. CIAPETTI, S. STEA, M. E. DONATI, G. ZINGHI, G. FONTANESI, R. ROTINI, L. MONTANARO, (1999) *J. Biomed. Mater. Res*. **47**:543
9. D. GRANCHI, L. SAVARINO, G. CIAPETTI, E. CENNI, R. ROTINI, M. MIETI, N. BALDINI, A. GIUNTI, *J. Bone Joint Surg*. **85B** (2003) 758
10. M. A. GERMAIN, A. HATTON, S. WILLIAMS, J. B. MATTHEWS, M. H. STONE, J. FISHER, E. INGHAM, *Biomater*. **24** (2003) 469
11. N. J. HALLAB, K. MERRITT, J. J. JACOBS, *J. Bone Joint Surg*. 83A (2001) 428
12. H-G. WILLERT, G. H. BUCHORN and A. FAYYAZI, in Proceedings of the Second International Conference on Metal-Metal Hip prostheses Past Performances and Future Directions, Montreal 2003
13. T. VISURI, E. PUKKALA, P. PAAVOLAINEN, P. PULKINEN, E. B. RISKA, *Clin. Orthop*. **329S** (1996) S280
14. C. P. CASE, V. G. LANGKAMER, R. T. HOWELL, J. WEBB, G. STANDEN, M. R. PALMER, A. J. KEMP, I. D. LEARMOUTH, *Clin. Orthop*. **329S** (1996) S269
15. A. T. DOHERTY, R. T. HOWELL, L. A. ELLIS, I. BISBINAS, I. D. LEARMOUTH, R. NEWSON, C. P. CASE, *J. Bone Joint Surg*. **83B** (2001) 1075
16. P. J. FIRKINS, J. L. TIPPER, E. INGHAM, M. H. STONE, R. FARRAR, J. FISHER, *J Biomech*. **34** (2001) 1291
17. P. J. FIRKINS, J. L. TIPPER, M. R. SAADATZADEH, E. INGHAM, M. H. STONE, R. FARRAR, J. FISHER, *Bio-Med. Mater.Eng*. **11** (2001) 143–157
18. J. E. NEVELOS, E. INGHAM, C. DOYLE, R. M. STREICHER, A. B. NEVELOS, W. WALTER, J. FISHER, *J. Arthro*. **15** (2000) 793
19. T. D. STEWART, J. L. TIPPER, G. INSLEY, R. M. STREICHER, E. INGHAM, J. FISHER, *J.Biomed. Mater. Res*. **66B** (2003) 567
20. S. WILLIAMS, T. D. STEWART, M. H. STONE, E. INGHAM, J. FISHER, *J. Biomed. Mater. Res*. **70B** (2004) 233
21. J. L. TIPPER, A. HATTON, J. E. NEVELOS, G. INSLEY, R. M. STREICHER, C. DOYLE, A. A. NEVELOS, *J. Fisher, Biomat*. **23** (2002) 3441
22. I. CATELAS, J. D. BOBYN, J. B. MEDLEY, J. J. KRYGIER, D. J. ZUKOR, A. PETIT, O. L. HUK, *J. Biomed. Mater. Res*. **55** (2001) 320
23. I. CATELAS, J. D. BOBYN, J. B. MEDLEY, J. J. KRYGIER, D. J. ZUKOR, A. PETIT, O. L. HUK, *J. Biomed. Mater. Res*. **55** (2001) 330
24. M. J. YANEZ, S. E. BARBOSA, *Micr Res. Tech*. **61** (2003) 463
25. P. S. BARBOUR, M. H. STONE J. F. FISHER, *Proc. Instn. Mech. Engrs*. **213** Part H (1999) 455
26. J. B. MATTHEWS, A. A. BESONG, T. R. GREEN, M. H. STONE, B. M. WROBLEWSKI, J. FISHER, E. INGHAM, *J. Biomed. Mater. Res*. **52** (2000) 296
27. J. M. LEE, E. A. SALVATI, F. BETTS, E. F. DICARLO, S. B. DOTY, P. G. BULLOUGH, *J. Bone Joint Surg*. **74B** (1992) 380
28. H. G. WILLERT, G. H. BUCHHORN, D. GOBEL, G. KOSTER, S. SCHAFFNER, R. SCHENK, M. SEMLITSCH, *Clin. Orthop*. **329S** (1996) S160
29. P. F. DOORN, P. A. CAMPBELL, H. C., *Amstutz, Clin. Orthop*. **329S** (1996) S206
30. K. G. SHEA, G. A. LUNDEEN, R. D. BLOEBAUM, K. N. BACHUS, L. ZOU, *Clin. Orthop*. **338** (1997) 219
31. G. BUSCHER, G. TAGER, B. DUDZINSKI, B. GLEISING, M. A. WIMMER, A. FISCHER, *J. Biomed. Mater. Res* **72B** (2004) 206